Urban Dark Fiber Distributed Acoustic Sensing for Bridge Monitoring

Julie Rodet, Benoit Tauzin, Mohammad Amin Panah, Philippe Guéguen, Destin Nziengui Bâ, Olivier Coutant, Stéphane Brûlé

Structural Health Monitoring

Urban Dark Fiber Distributed Acoustic Sensing for Bridge Monitoring

Journal:	*Structural Health Monitoring*
Manuscript ID	SHM-23-0615.R1
Manuscript Type:	Original Manuscript
Date Submitted by the Author:	04-Dec-2023
Complete List of Authors:	RODET, Julie; Laboratoire de Géologie de Lyon Terre Planètes Environnement, Université Claude Bernard Lyon 1, Ecole Normale Supérieure de Lyon, CNRS, Université Jean Monnet TAUZIN, Benoit ; Laboratoire de Géologie de Lyon Terre Planètes Environnement, Université Claude Bernard Lyon 1, Ecole Normale Supérieure de Lyon, CNRS, Université Jean Monnet Amin Panah, Mohammad; Laboratoire de Géologie de Lyon Terre Planètes Environnement, Université Claude Bernard Lyon 1, Ecole Normale Supérieure de Lyon, CNRS, Université Jean Monnet Guéguen, Philippe; Institut des Sciences de la Terre, Université Grenoble Alpes, Université Savoie Mont-Blanc, CNRS, IRD, Université Gustave Eiffel Nziengui Ba, Destin ; Institut des Sciences de la Terre, Université Grenoble Alpes, Université Savoie Mont-Blanc, CNRS, IRD, Université Gustave Eiffel, FEBUS Optics Coutant, Olivier; Institut des Sciences de la Terre, Université Grenoble Alpes, Université Savoie Mont-Blanc, CNRS, IRD, Université Gustave Eiffel BRULE, Stéphane; Menard
Keywords:	Bridge, Modal analysis, Urban area, Monitoring, Telecom fiber, Distributed Acoustic Sensing (DAS)
Abstract:	Distributed Acoustic Sensing (DAS) technology applied to telecommunication fiber optic networks offers new possibilities for Structural Health Monitoring (SHM). The dynamic responses of five bridges are extracted along a 24 km long optical fiber crossing the Lyon metropolitan area in France. From their characteristics signals, three physical parameters informing on the health of structures have been determined: vibration frequencies, damping and modal shapes. The fiber measurements are in agreement with velocimetric data serving as reference. The telecom optical fiber records the dynamic response of bridges in several directions and thus allows the reconstruction of 3D deformation modes using their orthogonality properties. Time tracking of frequencies, commonly used to assess structural integrity, shows that the average values of natural frequencies vary cyclically between day and night. The increase in frequencies during the night does not exceed 2% and probably reflects an overall stiffening of the structures due to the drop in temperature. The telecom fiber allows to obtain deformation

	and damping identity of structures, highlighting soil-structure coupling between the bridge and underlying soil. This study shows that it is possible to assess the spatial and temporal variability of bridge dynamic response from DAS data using existing fiber networks.

Urban Dark Fiber Distributed Acoustic Sensing for Bridge Monitoring

Julie Rodet[1], Benoit Tauzin[1], Mohammad Amin Panah[1], Philippe Guéguen[2], Destin Nziengui Bâ[2,3], Olivier Coutant[2], Stéphane Brûlé[4]

[1] LGLTPE - Université Claude Bernard Lyon 1, Ecole Normale Supérieure de Lyon, CNRS, Université Jean Monnet, Villeurbanne, France

[2] ISTerre - Université Grenoble Alpes, Université Savoie Mont-Blanc, CNRS, IRD, Université Gustave Eiffel, Grenoble, France

[3] FEBUS Optics, Pau, France

[4] Ménard, Chaponost, France

Abstract

Distributed Acoustic Sensing (DAS) technology applied to telecommunication fiber optic networks offers new possibilities for Structural Health Monitoring (SHM). The dynamic responses of five bridges are extracted along a 24 km long optical fiber crossing the Lyon metropolitan area in France. From their characteristics signals, three physical parameters informing on the health of structures have been determined: vibration frequencies, damping and modal shapes. The fiber measurements are in agreement with velocimetric data serving as reference. The telecom optical fiber records the dynamic response of bridges in several directions and thus allows the reconstruction of 3D deformation modes using their orthogonality properties. Time tracking of frequencies, commonly used to assess structural integrity, shows that the average values of natural frequencies vary cyclically between day and night. The increase in frequencies during the night does not exceed 2% and probably reflects an overall stiffening of the structures due to the drop in temperature. The telecom fiber allows to obtain deformation and damping identity of structures, highlighting soil-structure coupling between the bridge and underlying soil. This study shows that it is possible to assess the spatial and temporal variability of bridge dynamic response from DAS data using existing fiber networks.

Keywords: Distributed Acoustic Sensing (DAS) – Monitoring – Modal analysis – Telecom fiber – Bridge – Urban area

1. Introduction

The recent collapse of several bridges such as the Morandi Bridge in Genoa in 2018 (Calvi et al., 2019) and the Florida International University Pedestrian Bridge (Cao et al., 2020) has highlighted the need for society to devise monitoring strategies to prevent such failures (Figueiredo and Brownjohn, 2022). Failure often occurs due to design flaws, inadequate materials, overloading, or maintenance. Following the Morandi bridge collapse, nearly 35 000 French structures were diagnosed as being in poor structural condition and requiring close inspection (Maurey et al., 2019). Depending on operational conditions (Jacobsen et al., 2007; Chen et al., 2021; Anastasopoulos et al., 2021) and types of damage (Hearn and Testa, 1991; Khoo et al., 2004; Ernst et al., 2022), Operational Modal Analysis (OMA) based on periodic or continuous measurements with sensor networks (Brownjohn et al., 2010; Magalhães et al., 2008) can be a suitable solution for anomaly detection and early warnings before a potential collapse (Doebling et al., 1996; Peeters and De Roeck, 2001; Farrar et al., 2001; Farrar and Worden, 2007). Most of the sensors currently in use are point sensors, such as inclinometers, velocimeters, accelerometers and extensometers, with maximum sampling lengths of a few tens of meters. These technologies are laborious to implement when it comes to multiplying measurement points over kilometers of linear length (Glisic and Inaudi, 2012; Rizzo and Milazzo, 2021), or to achieve very high spatial sampling on particularly stressed structures subject to earthquakes, extreme environmental conditions, or significant traffic load such as motorway bridges (Gara et al., 2019). In urban environments, the installation of such sensors, dedicated to monitoring, can also prove difficult due to the density and complexity of the layout (various traffic, transport infrastructures, buildings) (Snover et al., 2021).

Distributed Acoustic Sensing (DAS) technology is an emerging alternative offering new observational possibilities, by giving easy access to hundreds to thousands of data points along telecom optic fiber networks (Jousset et al., 2018; Ajo-Franklin et al., 2019). This technology consists in making laser scattering measurements on an optical fiber to estimate the deformation of the cable associated with environmental vibrations. Initially developed for the oil and gas industry for detecting leaks along pipelines (Tanimola and Hill, 2009), building vertical seismic profiles in wells (Mestayer et al., 2011; Hartog et al., 2014) and doing reservoir monitoring (Johannessen et al., 2012; Mateeva et al., 2014), this technology is now exploited in various applications for fault detection (Jousset et al., 2018; Wang et al., 2018), subsurface imaging (Ajo-Franklin et al., 2019), statistical analysis of road traffic (Van den Ende et al., 2022; Song et al., 2021), ambient noise analysis (Dou et al., 2017; Zeng et al., 2017), and studying the

interaction of ocean masses with the solid Earth (Hartog et al., 2018; Lindsey et al., 2019; Sladen et al., 2019). We use here the technology in the frame of the Distributed Acoustic Sensing Auvergne Rhone-Alpes (DASARA) project, to characterize the urban seismic environment.

The main goal of this study is to assess the effectiveness of utilizing dark fiber, which refers to non-illuminated fiber for internet data transfer, in monitoring spatially distributed bridges within an urban setting using modal-based methods (Cunha et al., 2018). To achieve this, we conducted Operational Modal Analysis (OMA) on five bridges using DAS data. The DAS data was continuously collected over 53 hours at a distance from the structures, covering a 24km urban telecommunication dark optical fiber. To determine the utility of urban fiber optics for structural monitoring, we compared the results obtained from the DAS measurements with independently acquired velocimetric data from one of the five bridges.

After a description of the experiment in section 2, we outline in section 3 the numerical methods used to extract modal parameters from the experimental data. Then, we present in section 4 the results of the comparison between the two types of data (DAS and velocimeters) for one bridge, before showing the results of the OMA performed on the other bridges along the interrogated fiber (section 5). Finally, we interpret our results in section 6 and highlight the main conclusions of the study in section 7.

2. A 24 km-long urban optical fiber experiment

With a population nearing 1.33 million, the Lyon metropolitan area is advancing its smart city capabilities through a network encompassing over 900 km of optical fiber and 14 operator access points (Figure 1a). In this study, the DAS interrogator was linked to the fiber at an operator access point (POP) in the northwest. The dark fiber utilized here is a G657-A1 step-index single-mode telecom fiber, a specification set by the International Telecommunications Union (ITU). It is designed to function at 1310nm or 1550nm and features a 9µm diameter silica core, allowing light to travel extensive distances without requiring re-amplification. To preserve signal quality across long distances, this fiber type minimizes chromatic dispersion and signal losses through attenuation; specifically, the attenuation is less than 0.2dB per km for the 1550nm wavelength employed in this experiment.

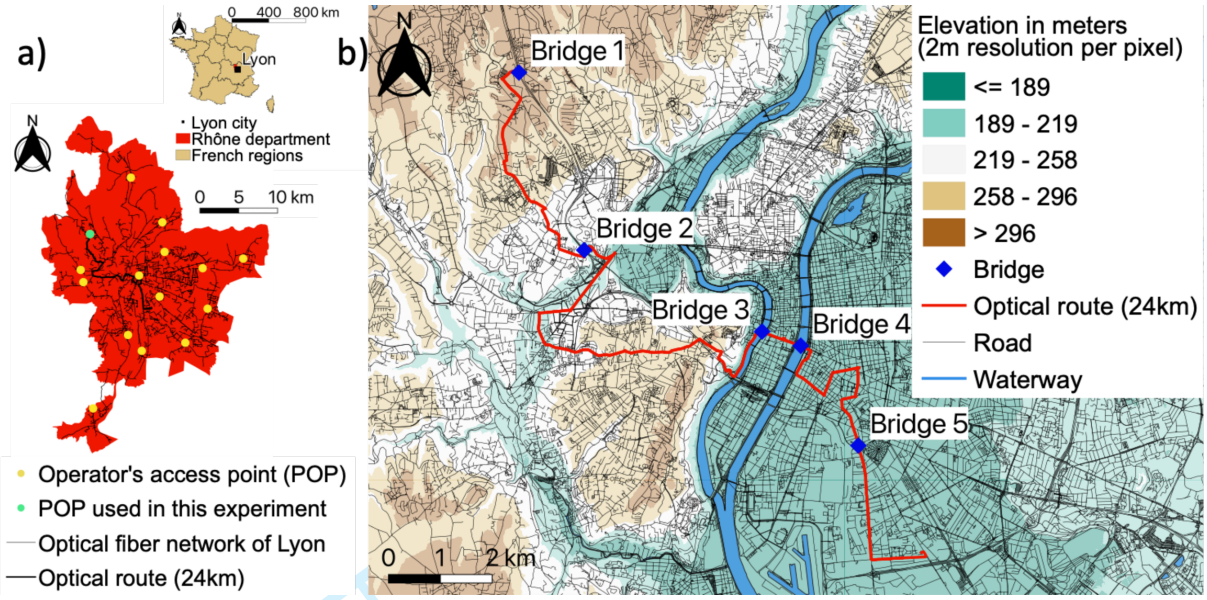

Figure 1: a) Map displaying the Lyon fiber network in black and highlighting fiber access points in the Lyon metropolitan area in yellow. The green dot denotes the access point used in the initial DASARA experiment. b) Map illustrating the region's topography, optical path, and the position of the structures. The access point is situated near Bridge 1 in the northwest. This map was generated using the Density Analysis plugin of the geographic information system software QGIS (Quantum GIS) and a DTM made available from the Metropole of Lyon. The DTM was generated in 2018 from raw data (slope break lines and points on the ground) on the territory of the Metropole of Lyon with a resolution of 2m per pixel.

DAS data are acquired along the 24 km of optical fiber (Figure 1b), sampling three types of geology, three different urban fabrics and five bridges. The raw data are dominated by transient signals associated with road traffic, as well as high-amplitude quasi-stationary bands associated with bridges over the A6 Lyon-Paris highway and the Saône and Rhône rivers (Figure 2c,d).

Telecom optical fiber is passed through technical ducts of bridge decks. Bridges 1 and 2 are similar road bridges with prestressed concrete girders: the first one is 64 meters long and has 5 spans, the second one is 56 meters long and has two spans. Bridge 3 is also in prestressed concrete, but with a 124-metre-long arch structure comprising three arches: a large 67.50-metre central arch and two 25.75-metre lateral arches (Figure 2a). A special feature of this bridge is its decorative ashlar cladding. Unlike the previous ones, Bridge 4 is a steel box girder bridge with a total length of 205 meters and three spans. Finally, Bridge 5 is a small, 35-meter-long prestressed concrete frame bridge. Bridges 1, 2 and 5 date from the 1970s, while bridges 3 and 4 date from the 1950s.

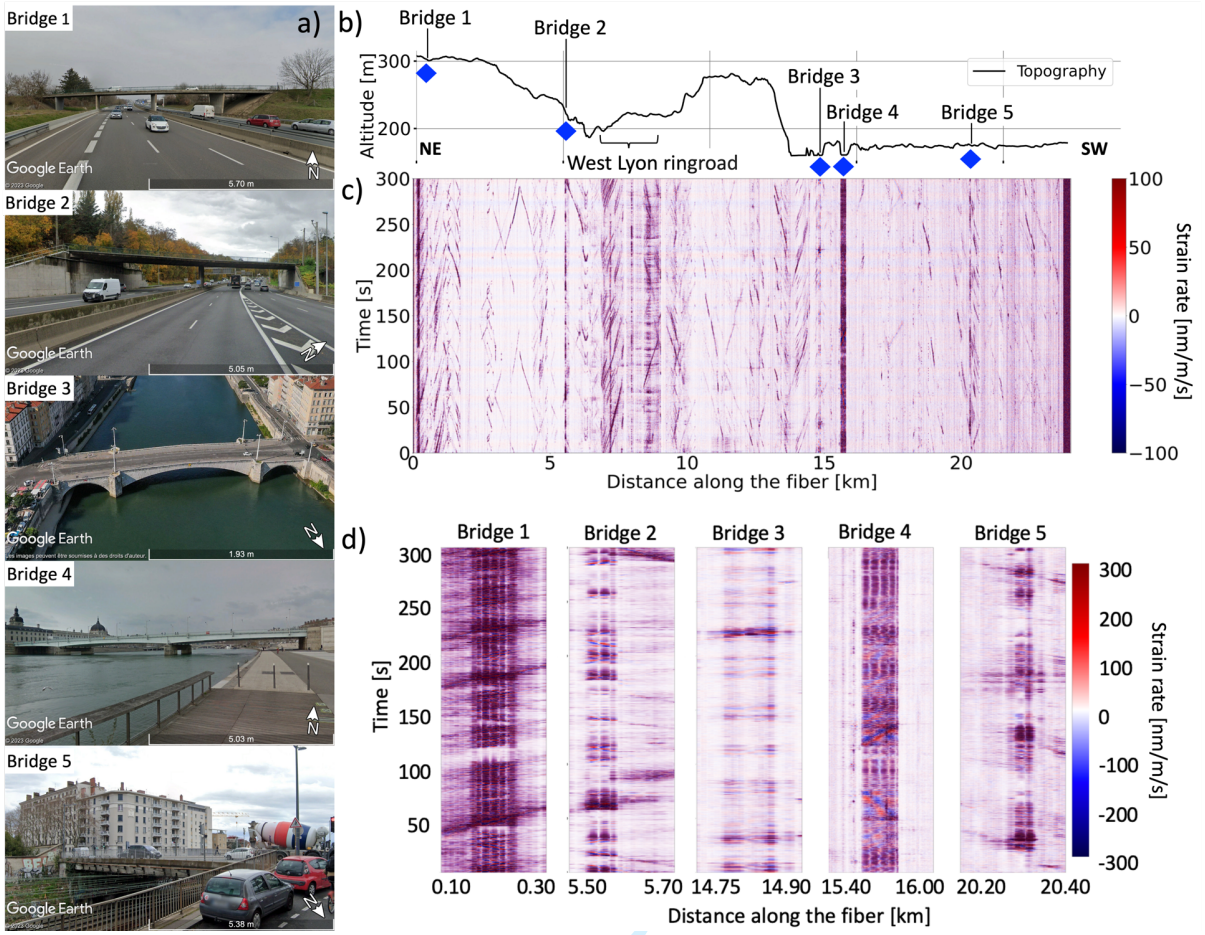

Figure 2: a) Photo of each instrumented bridge. b) Vertically exaggerated topographic profile extracted along the 24 km of fiber. c) 5 minutes of strainrate data along the 24 km of fiber. The strainrate corresponds to the time derivative of the strain and is expressed in nm/m/s. d) 5 minutes-long sections of strainrate data emphasizing the signals from the five bridges. Bridge 1: Highway Paisy (A6), Bridge 2: Interchange (A6), Bridge 3: Saône river, Bridge 4: Rhône river, Bridge5: Railway.

3. Materials and Methods

Ambient vibration recordings offer a reliable and consistent source of dynamic information regarding structural behavior (Peeters and De Roeck, 2001; Magalhães et al., 2008). The main sources of structural excitation include traffic on the deck and ambient anthropogenic noise, such as external traffic, construction activities, and industrial operations, as well as natural elements like wind and earthquakes. Particularly, ambient vibration recordings enable the estimation of dynamic parameters associated with variations in the

physical properties of the structure (De Roeck et al., 2003; Xia et al., 2003; Cunha and Caetano, 2006). Consequently, they serve as a valuable tool for monitoring the condition of structures (Farrar et al., 2001; Magalhães et al., 2012).

3.1 DAS acquisition

By sending high-frequency laser pulses into the fiber, an optoelectronic interrogator unit records and analyzes the backscattered light from heterogeneities along the cable (Tanimola and Hill, 2009). The silica constituting the core of the telecom optical fiber contains defects inherent to the manufacturing process. These heterogeneities disturb the flow of photons and reflect part of the light according to the principle of Rayleigh scattering. Since it is related to defects in the structure of the optical fiber, Rayleigh backscattering is repetitive all along the optical fiber (Froggatt et al., 2004). When the fiber is disturbed by an external event (passage of a car, an earthquake, etc.), the fiber locally deforms, in compression or dilatation. This introduces a phase shift in the backscattered light (e.g. Fichtner et al. 2022), and the scattering spectrum of the fiber is modified accordingly (Gifford et al., 2007). This phase shift makes it possible to locate and measure the variation of the physical parameter at the origin of the disturbance. In our experiments, we use an optoelectronic interrogator unit FEBUS A1-R from the FEBUS Optics company.

The optical phase shift between two positions along the optical fiber is linked to the longitudinal strain applied to the fiber through the following equation:

$$\varepsilon_{yy} = \frac{\lambda . d\theta}{4\pi . n . GL . \xi} \qquad \text{(Eq. 1)}$$

where ε_{yy} is the longitudinal strain, λ is the optical wavelength, $d\theta$ is the phase shift, n is the optical fiber index, and ξ is a correction factor. The measurement of optical phase shift is obtained along an integration distance called the gauge length (GL). The main acquisition parameters are the length l of the interrogated fiber, the frequency f of the interrogation pulses (giving the temporal sampling interval), the spatial sampling interval Δx, and the gauge length GL to optimize the optical signal. These parameters must be adjusted according to the signal to be detected, as well as the acquisition rate to guarantee the integrity of the recorded data.

Generally, the gauge length should be less than the wavelengths of the acoustic signal of interest. The smaller the gauge length, the finer the spatial sampling and, in theory, higher frequency bridge deformation modes can be measured. But the smaller the gauge length, the

higher the noise level in the data because the strain measurement is integrated over a smaller distance. As a compromise, we opted for a gauge length of 10m and a spatial sampling interval of 5m, enabling the extraction of the bridges' dynamic characteristics. The data were collected in strain rate ($nm.m^{-1}.s^{-1}$) at a sampling frequency of 400Hz and subsequently resampled at 100Hz before undergoing digital processing.

3.2 LE-3D/5s MkIII sensors and CityShark acquisition

To assess the significance of the measurements taken on the bridges with the telecom fiber, these are compared with conventional measurements. Fifteen-minute-long measurements are taken along the deck of the Bridge 1 using a Cityshark acquisition system (Chatelain et al., 2012) and four velocimeters LE-3D/5s MkIII (Figure 3a), over rolling positions every 4 meters to mimic synchronous measurements of structure deformation (see procedure given by Michel et al., 2010). The first horizontal component of the velocimeters is placed in the direction of the longitudinal axis of the bridge, assuming that the fiber is oriented along this axis. These conventional data have been acquired with a sampling frequency of 200Hz.

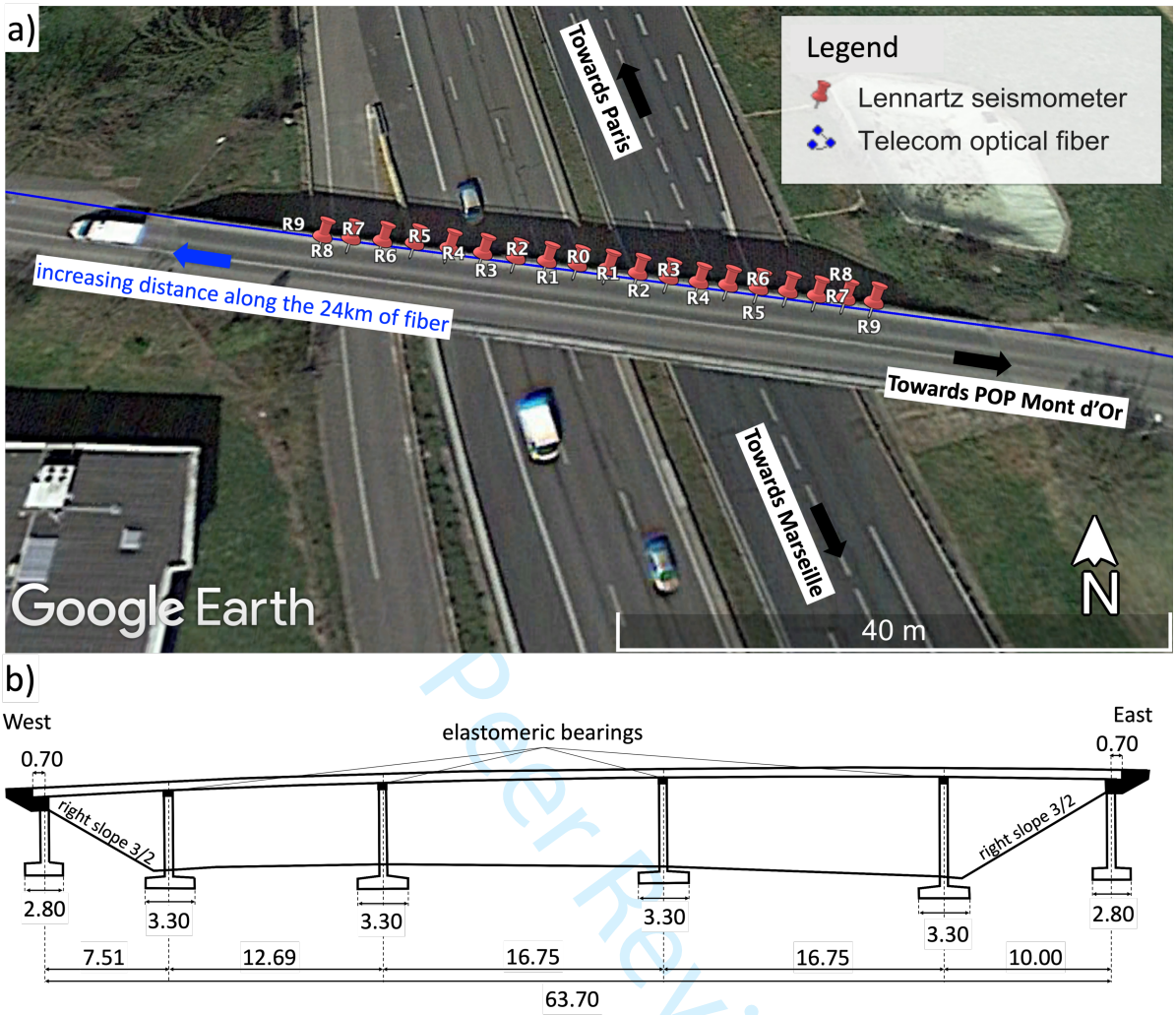

Figure 3: a) Satellite image of the Bridge 1 (Paisy bridge) crossing the A6 highway, with the positions of the velocimeters used to acquire conventional measurements. b) Longitudinal section of the Bridge 1 (modified from a plan of the Ministry of Equipment, Rhône Department, Boussiron Company). The dimension is given in meters.

3.3 Postprocessing

3.3.1 Power Spectral Density

To perform the comparison between conventional data and the fiber data, power spectral density (PSD) functions are calculated using the Welch's method (Welch, 1967) (Figure 4). Spatial variations in frequency along the bridges (Figure 5) are estimated from PSDs computed over the 53h of data with 50% overlap in time, to reduce the error of the PSD estimate. From the PSDs, we perform temporal tracking of bridge responses and modal frequencies (Figures 6

and 7). For frequency monitoring, the 53h data are segmented into half-hour portions. Then, the PSDs are calculated for the 15 2-minute-long windows of each half-hour without overlap.

3.3.2. Singular Value Decomposition

We decompose the dynamic response of structures into independent orthogonal eigenvectors using singular value decomposition (SVD) (Rao, 1973,). SVD provides the eigenmodes of the structure, useful to identify modes that are very close in frequency and detect changes in vibration modes of the structure (Magalhaes and Cunha, 2011). The SVD is applied to a matrix comprising all the spectra along a bridge evaluated at all discrete frequencies between 0 and 50 Hz. SVD enables us to reduce the dimension of the data and facilitate its visualization. The eigenvectors shown in section 5 are associated with the highest singular value and represent the dominant vibration modes of the bridge.

3.3.3 Random Decrement Technique

The damping coefficient of the bridge structure is calculated using the random decrement method (RDT) (Cole, 1973). Based on the principle that the response of a system to any loading consists of three parts – the response to an initial displacement, the response to an initial velocity and the response to a random load between the initial state and time t - this technique consists on averaging a large number of segments of the temporal response of the system with the same initial conditions (Mikael et al., 2013). By erasing the random component of the analyzed signal, this technique therefore allows access to the response of the system due to the initial conditions alone, also known as the impulse response or RD function. Averaging these time segments also helps to reduce the level of noise in the RD functions, which is particularly important as the measured structural responses are always partially noisy. We chose to look for all the places where the signal crosses zero to select the signal segments to be averaged (Rodrigues and Brincker, 2005).

In our study, the 53 hours of DAS data are divided into half-hour portions. One frequency and damping values are obtained per half-hour without overlapping windows. Then, the RDT method, described in Gueguen et al., 2016 and Brossault et al., 2018, is applied to each of the 30-minute portions, corresponding to more than 8000 periods of the first mode of Bridge 1 (around 4.6Hz). The calculation of the RD function assumes that each signal window of length τ is stationary. For each half-hour portion, N = 1800/5 = 360 windows are selected as

a minimum (without overlap). In practice, there is considerable overlap between each 5 s window, so N is greater than 500 windows, which is essential to obtain a stable and relevant estimate of the damping (Jeary, 1997). For each half hour, a RD function is obtained for each mode. This function is exponentially damped and satisfies the so-called logarithmic decrement of the damping (Clough and Penzien, 1993). The damping value ξ is obtained by performing a linear regression on the natural logarithm of $exp(-\xi\omega t)$, which corresponds to the envelope of the RD function. Before windowing and calculating the RD function, a bandpass filter is applied to the time signal. This filter is a 20% frequency band centered on each vibration mode. Each damping value is calculated in the middle of the structure assuming that the deformation is the most important there.

3.3.4. Operational Modal Analysis

In our study, the shape of the vibration modes is reconstructed from both types of data (velocimeters and optical fiber) using the non-parametric SSI-COV method. The Stochastic Subspace Identification (SSI) method is a time domain method allowing the identification of modal parameters (Van Overschee and De Moor, 1996) and a variant of this method is the Covariance-Driven SSI (SSI-COV) algorithm (Magalhaes and Cunha, 2011). To calculate the modal shapes from the records, we use the Python implementation of the SSI-COV method from the CESSIPy module (Carini and Rocha, 2022).

3.3.5. Modal Assurance Criterion (MAC)

Correlation coefficients such as the modal assurance criterion (MAC) are often used to detect structural damage from the modal deformations of a structure (Allemang and Brown, 1982). This coefficient allows to evaluate the degree of correlation between two measured modal deformations. After validation of the modal shapes of Bridge 1 obtained with the fiber (Figure 8a, b), this MAC index is calculated between the first modal shape recorded (considered to be the reference) and the modal shapes of each half-hour during the 53 hours of recording. A coefficient of one represents a perfect correlation between the curves and no damage

3.3.6. Uncertainty estimates

The raw DAS signal is cut in half-hour windows, over which are estimated the frequencies through direct measurement, and the damping coefficient through the RDT method. In both cases, the uncertainties are calculated by constructing distributions of measurements through

the bootstrap resampling method (Efron and Tibshirani, 1991). To perform time tracking of frequencies and structural damping, a mean value and standard deviation are determined for each 30-minute signal window. For this purpose, 100 bootstrap samples per 30-minute window are created. Each sample is the result of randomly drawing 15 2-minute windows for the frequency measurement and a set of initial conditions (greater than 4000) for the damping measurement. For each sample, an average PSD or RD curve and a damping value are calculated. The measurement and error on the measurement are obtained from the average and standard deviation over the 100 bootstrap samples.

4. Comparison between conventional and DAS measurements

4.1 Characteristic spectral signature of the Paisy bridge

The singular value decomposition (SVD) of the seismic signal recorded at the center of Bridge 1 reveals two distinct characteristic modes at 4.6Hz and 6.0Hz, respectively. Notably, the frequency response exhibits clear distinctions between measurements taken on and outside the bridge for both data types. Despite uncertainties, the velocimetric and fiber-optic measurements consistently indicate identical frequency values for these predominant modes (see Figure 4). Additionally, at higher frequencies, other modes can be identified, aligning closely with velocimetric measurements. All these modes offer valuable insights for characterizing the dynamic response of the bridge, as discussed in section 4.4.

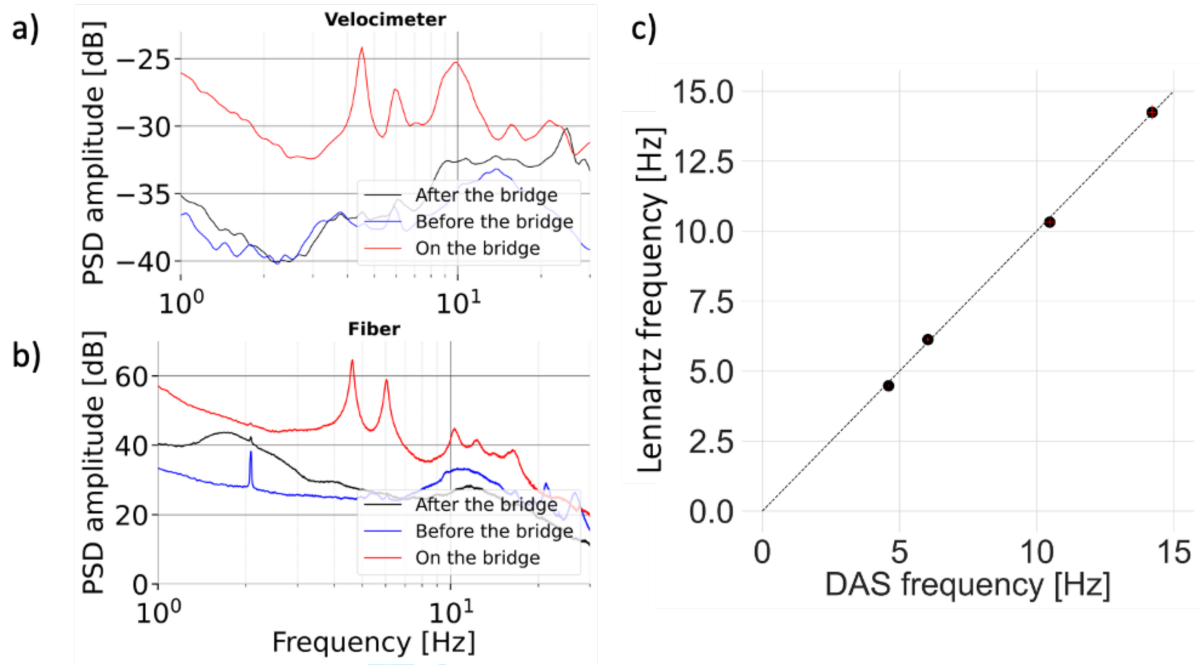

Figure 4: Fifteen minute PSDs of three traces obtained on the bridge (at the midpoint), after (152 meters beyond the west abutment) and before (60 meters before the east abutment) Bridge 1 (Paisy bridge) for the velocimeter a) and the telecom fiber b). a) Correlation diagram illustrating the relationship between velocimetric and fiber frequency measurements for the initial four vibration modes of Bridge 1. The uncertainties in red are smaller than the width of the measuring points shown in black.

4.2 Spatial variation of the Paisy bridge dynamic response

We evaluate the relevance of making measurements of the dynamic response of the bridge by exploiting the fine spatial sampling provided by the optical fiber. We use the velocimetric measurements for validation. Both data give consistent results for the modal frequencies and spatial variations of their relative amplitudes (Figure 5), despite differences in terms of spatial sampling. The two modes at 4.6 Hz and 6 Hz are clearly tracked along the bridge, both for fiber (Figure 5a) and velocimeter data (Figure 5b, d).

From the fiber data, the dynamic response of the abutments is identified and has a much wider frequency band (up to 30Hz) than the deck which is lower frequency (lower than 17Hz) (Figure 5a). This broadband response of the abutments is also observed on the velocimeter data, on the eastern side of the bridge (Figure 5b). The west abutment is not visible in the velocimetric data because we did not make enough measurement points in the western direction to observe it. Figure 5a and Figure 5b, c show areas where the spectral amplitude of the PSDs is attenuated

compared to the rest of the structure. These nodes can be considered as bearing areas, where there is less deformation and displacement due to the presence of the bridge piers. Compared to velocimeter measurements (Figure 5), the dynamic response of the structure seems to be equally well resolved with the fiber, even for the higher vibration modes. A better resolution could be obtained by decreasing the gauge length GL and the spatial resolution Δx in the DAS acquisition, and by decreasing the spacing of the velocimeters along the structure.

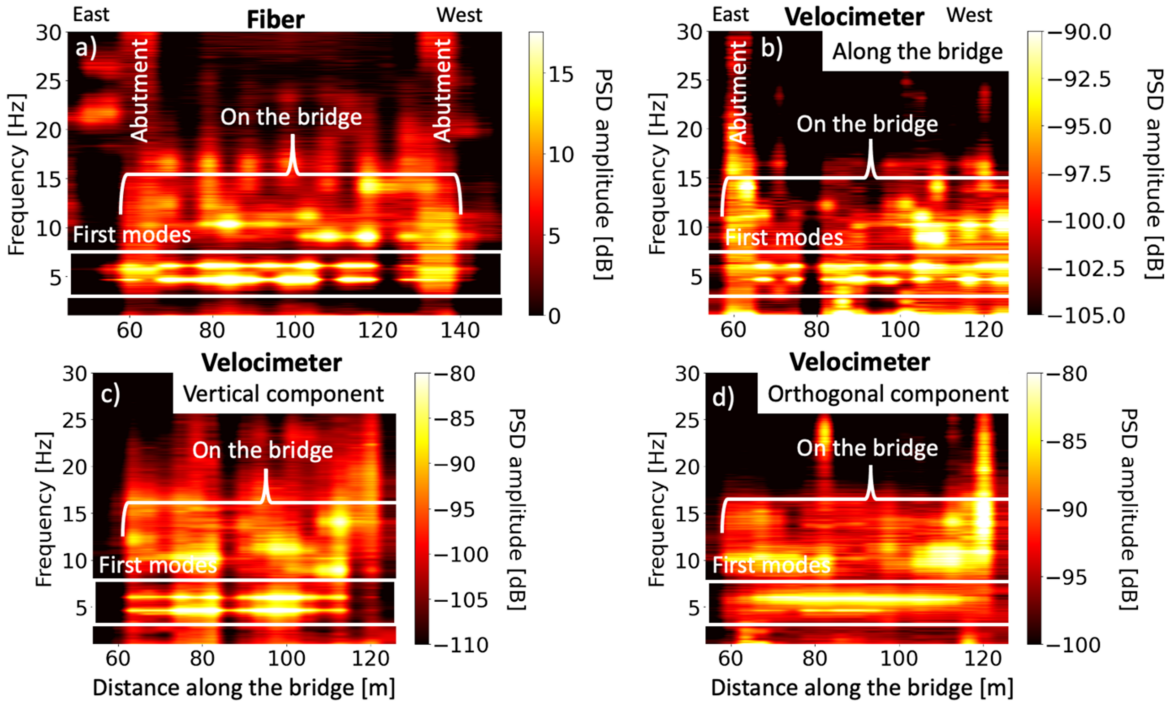

Figure 5: Spatial variations of the frequencies obtained for 15 minutes of recording from the telecom fiber a) and the three velocimeter components along the bridge b), in the vertical direction c) and orthogonal to the bridge d).

4.3 Temporal variation of the Paisy bridge dynamic response

We present in Figure 6 the temporal evolution of the dynamic response in the middle and outside the bridge 1 during the 53 hours of the DAS experiment. A clear day/night cycle appears, due to variations in the noise level originating from anthropic activity, mainly road traffic sources (Figure 6a, b). The noise level is much lower at night than during the day, and the dynamic response of the bridge can be observed continuously day and night (Figure 6b). The first clearly visible vibration modes are at 0.3, 4.6 and 6Hz. Other higher modes are visible

between 10 and 18Hz. A comparison of the two spectrograms shows that the traffic response between 25Hz and 35Hz appears to be amplified by the structure.

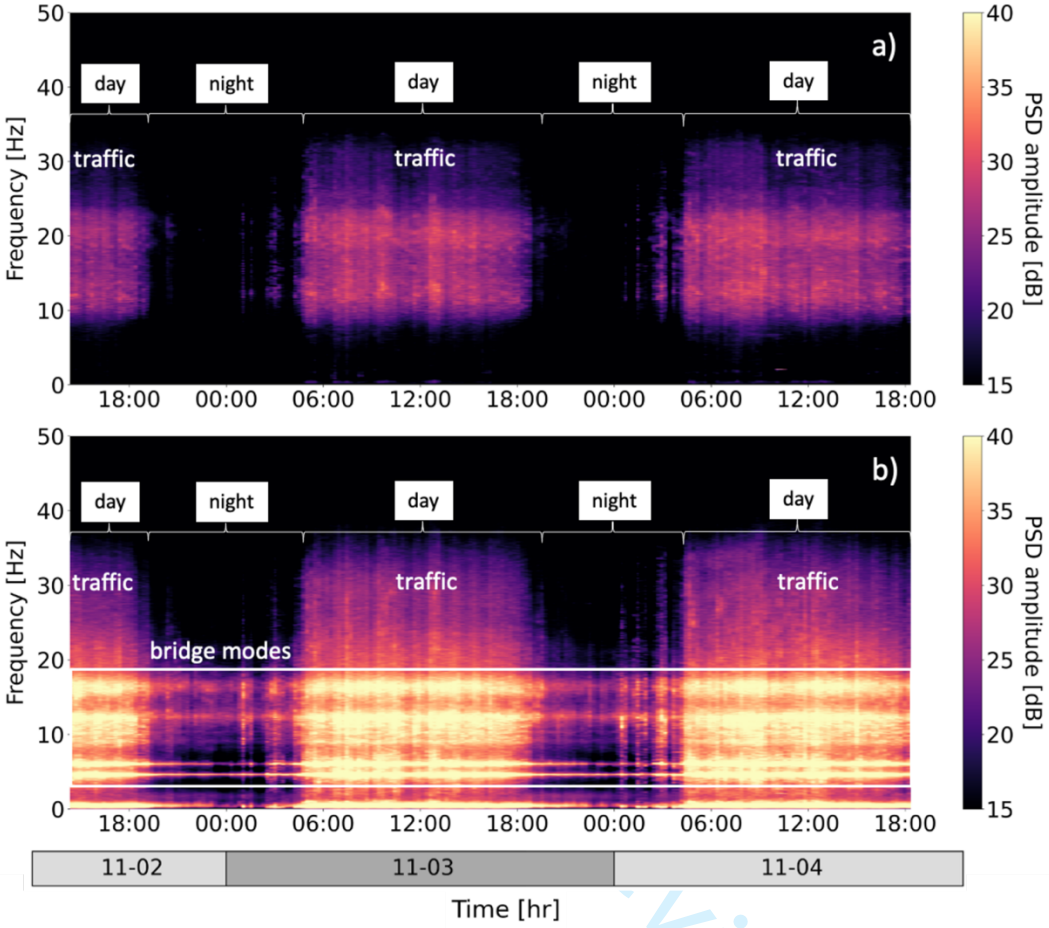

Figure 6: Spectrograms over 53 hours of data acquisition representing the temporal variations of anthropogenic activity and the cyclicity of the source a) outside (158 meters beyond the west abutment) and b) in the middle of the structure. The date in November is indicated in gray at the bottom. These spectrograms are obtained from the power spectral densities of the fiber signals.

In order to assess the stability of the dynamic measurements made with the telecom fiber, we observed the temporal variations of the natural frequencies and their respective amplitudes during the 53 hours of acquisition (Figure 7). We do not correct for the effet of temperature (see section 6.3). The frequencies of the first two modes vary by 0.0986Hz and 0.0852Hz respectively. The first mode therefore seems to be the most influenced by environmental conditions. Overall, these two modes follow a cyclic evolution with a slight increase in frequency during the night (Figure 7a, b).

Amplitudes vary over time, following the day/night cycle, and fluctuate with human activity (Figure 7c, d). The amplitudes increase during the day and decrease at night, which seems consistent with the fact that the traffic excites the bridge during the day (Figure 6). The amplitude variability of daytime measurements is larger than the one of nighttime measurements (Figure 7c, d).

We present in Figure 7e, f the damping measurements obtained from the RDT method in the middle of Bridge 1. Variations also tend to follow a day/night cycle, with a slight decrease during nighttime.

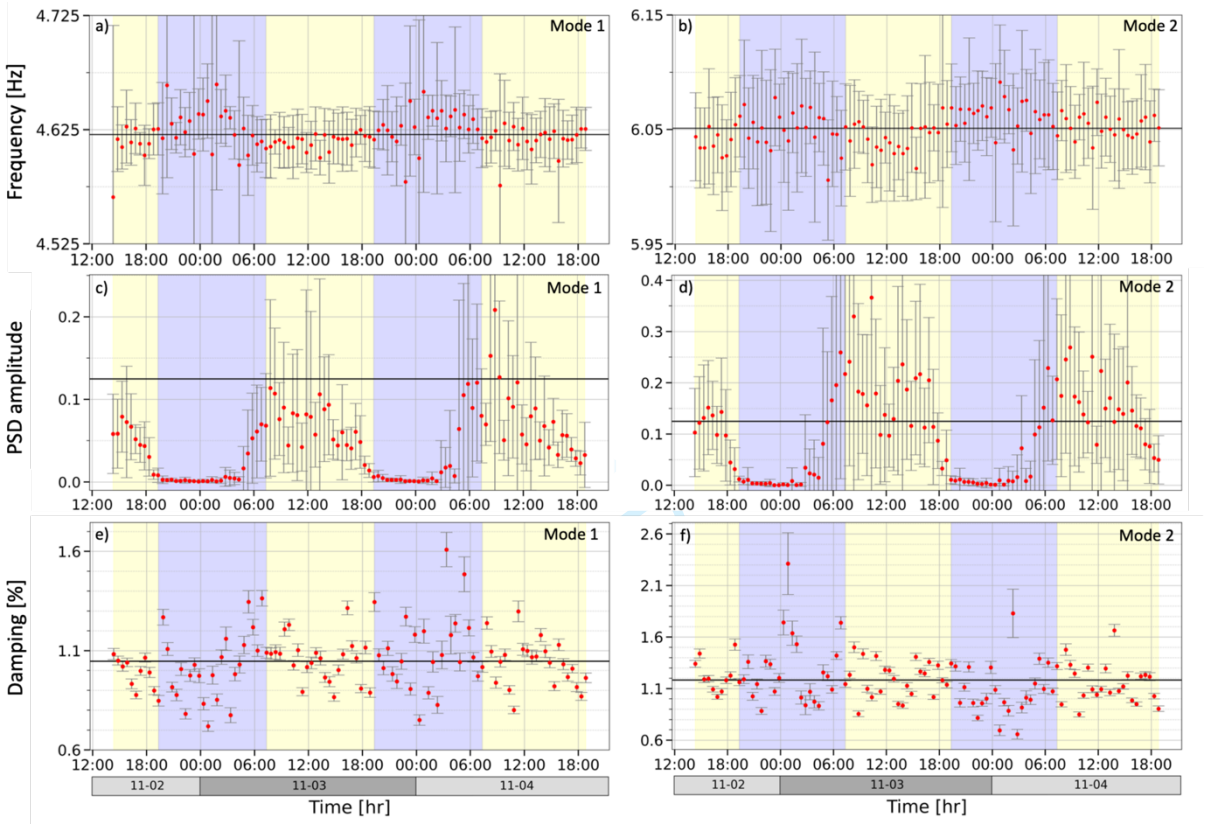

Figure 7: Temporal variations of the frequency, the amplitude and damping of the Paisy bridge from telecom fiber data for mode 1 a), c) and e) and mode 2 b), d) and f). Uncertainties are calculated using bootstrap resampling. Frequencies are measured on power spectral densities and damping is calculated using the RDT method.

4.4 Modal shapes of the Paisy bridge

Modal shapes for the two vibration modes at 4.6 and 6Hz are associated with two bending modes. Indeed, according to the velocimetric measurements, the 4.6Hz and 6Hz modes correspond to the first vertical (Y-Z plane) and transverse (X-Y plane) modes of the structure

respectively. With the fiber, the same modal shapes are identified with the position of the five spans and the bridge piers blocking the vertical movement (Figure 8). In both types of data, the amplitude of the vertical mode is higher on the western span than on the eastern span (Figure 8a). In contrast, the transverse mode is more symmetrical and its oscillations are more regular (Figure 8b). For higher modes, the difference in space sampling for the velocimeter and the DAS provide the largest differences in modal shapes. Because of its continuous space sampling, DAS solution is much more efficient than velocimeters for mode shape reconstruction.

Figure 9 shows some variations in the value of the MAC index during the DAS acquisition. Occurring mainly at night, these variations are transient and their amplitude does not exceed 0.01. MAC indices tend to decrease during the night and then rise and stabilize during the day. The decreases in observed MAC index cannot be associated with damage to Bridge 1 because they are not irreversible (Gueguen and Tiganescu, 2018). These variations reflect a change in the dynamic behavior of the bridge during the night, and seem to be correlated with variations in other modal parameters (Figure 7).

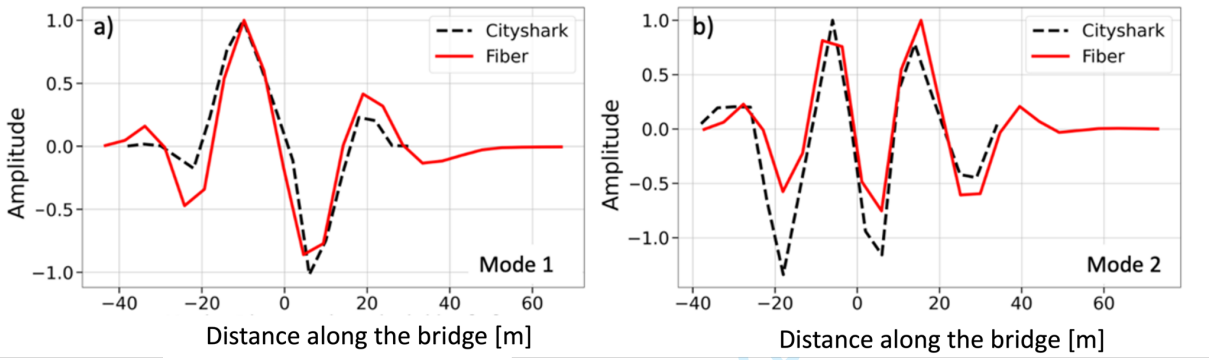

Figure 8: Modal shapes obtained with the SSI-COV method for the two first modes of Bridge 1 from the data recorded by the velocimeters and telecom fiber.

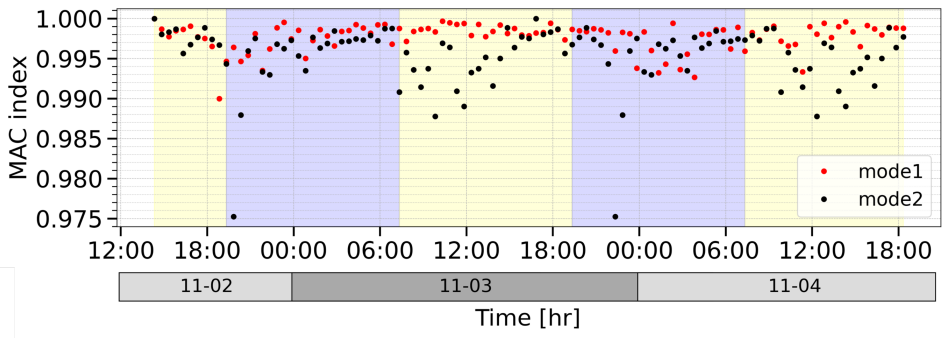

Figure 9: Variations in the MAC index over the 53 hours of acquisition for the Bridge 1. The MAC index is calculated every half-hour in relation to the reference modal deformation, corresponding to the first half-hour of acquisition.

5. Dynamic responses of the five bridges from a single DAS acquisition

Following the validation of fiber measurements on Bridge 1 through comparison with velocimetric data, we extended our analysis to the four other bridges situated along the same optical path. Modal characteristics such as natural frequencies, damping, and modal shapes were extracted and are presented in Figures 10-12.

Bridges 2, 3, and 5 are reinforced, pre-stressed concrete structures with approximately 60 meters in length, resulting in vibrational signatures akin to that of Bridge 1 (see Figure 10). Notably, the first modes of Bridge 3 exhibit a less distinct double peak compared to Bridges 1, 2, and 5 (Figure 10b). Unlike the others, Bridge 3 is an arch bridge with a white Hauteville stone cover (Figure 12a). This architectural feature could explain the deviation in its signature, especially if the fiber is routed between the concrete frame and the stone cover.

In contrast, Bridge 4 is a 205-meter-long steel bridge with a unique vibrational signature reflecting multiple resonances attributed to its extended length and construction materials (Figure 10). Given its greater length, the first vibration modes of Bridge 4 have significantly lower frequencies than the other bridges (refer to Table 1), making it the most flexible structure in this study. Notably, in Figure 10a, the two frequency bands associated with the abutments of Bridge 1 are not consistently visible for all bridges. While the western abutment is discernible for bridges 2 and 3, it is less clear for bridges 4 and 5. This variation could stem from differences in the environment, such as soil conditions, design, or vibration source. However, the nodal positions with minimal deformations and the alignment of piers along the deck are evident for all five bridges (Figure 10a).

On the bridge SVDs (Figure 10b), a broad peak is observed at low frequencies between 0.1 and 0.3 Hz. This mode appears to be physical, as it is also visible in the spectra calculated from the velocimetric data for Bridge 1. We hypothesize that this mode corresponds to the secondary peak of the microseismic noise.

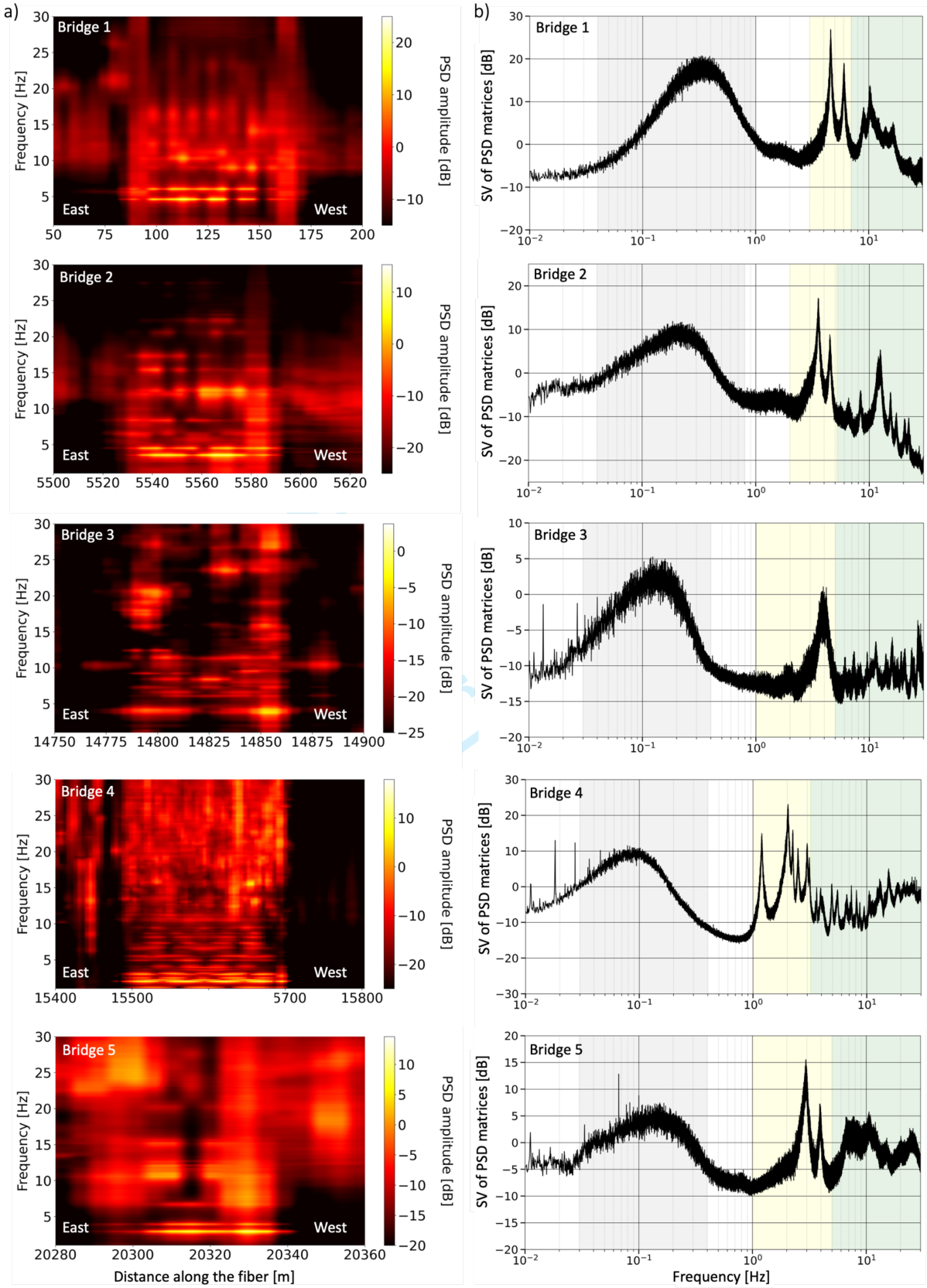

Figure 10: a) Spatial variations and b) SVD of the dynamic response of the five bridges . Bridge 1: Paisy; Bridge 2: A6; Bridge 3: Saône; Bridge 4: Rhône; Bridge 5: Railway.

In contrast to other bridges, Bridges 3 and 5 exhibit a first mode that is more damped than the second, as outlined in Table 1. It is noteworthy that the damping values derived from velocimetric measurements consistently appear slightly lower than those obtained from fiber measurements, with a difference ranging from 0.03% to 0.04% for the first mode and up to 0.09% for the second mode (refer to Table 1). Additionally, minor variations of less than 0.05 Hz are evident between the two types of recorded frequencies.

Given the asynchronous nature of the two measurement methods, differences in environmental conditions, particularly excitation sources and temperatures, could account for these disparities in frequencies and damping.

Name of the bridge	Telecom fiber				Lennartz sensors			
	ksi1 [%]	ksi2 [%]	fr1 [Hz]	fr2 [Hz]	ksi1 [%]	ksi2 [%]	fr1 [Hz]	fr2 [Hz]
Bridge 1 (Paisy)	1.07	1.22	4.61	6.02	1.04	1.13	4.56	5.99
Bridge 2 (A6)	1.54	1.78	3.54	4.50	-	-	-	-
Bridge 3 (Saône)	2.03	1.21	4.10	6.11	1.99	1.17	4.10	6.13
Bridge 4 (Rhône)	1.08	3.78	1.19	2.03	-	-	-	-
Bridge 5 (Rail)	2.27	1.97	2.86	3.89	-	-	-	-

Table 1. Mean frequencies (fr1, fr2) and damping (ksi1, ksi2) of the first two modes for the five bridges studied.

The spectrograms presented in Figure 11a showcase the fiber's capability to concurrently monitor the frequencies of five bridges in a single continuous acquisition over time. Similar to Figure 7, the vibration modes of different bridges and the influence of traffic are observed. The frequency monitoring across the five bridges (Figure 11b) reveals a distinct day/night cycle. Given that all five bridges are located within the same geographical area, it can be presumed that these variations stem from temperature changes between day and night, as this environmental factor significantly influences the dynamic response of structures (Peeters and De Roeck, 2001).

The most considerable frequency variations occur for the first two modes of bridges 3 and 5, ranging between 0.15 and 0.22Hz. For bridges 1 and 5, the first mode exhibits more variation than the second, contrary to bridges 2, 3, and 4, where the second mode experiences more significant changes. Hence, the cyclic variations observed affect modes differently based on the structure type and its environment. Notably, uncertainties in the frequency measurements for bridge 3 are larger than those for other bridges. Due to noisier and less distinct SVD peaks (Figure 10b), the frequencies measured on the spectra for each bootstrap sample are more

dispersed, resulting in increased uncertainties. Nevertheless, uncertainties in frequency measurements obtained through bootstrap resampling remain consistent throughout the 53 hours (Figure 11b) and do not appear influenced by shifts in environmental conditions.

Figure 12a displays the modal shapes for the first two modes of each structure. The position of nodes and antinodes enables clear identification of spans and pier positions. Notably, for bridges 1, 2, and 4, the shapes of the second modes are more symmetrical than those of the fundamental modes. The amplitude of the fundamental mode for bridge 2 is more pronounced on the eastern span, closest to the fiber's origin (POP). Conversely, the fundamental mode shape of bridge 4 has a slightly larger amplitude on the third span to the west of the structure. Bridge 3's fundamental mode shape appears distorted compared to the other bridges, attributed to its non-girder bridge structure. Additionally, bridge 5 stands out with the peculiarity that its first two modes exhibit nearly identical modal deformations. It is important to note that, with the uniaxial nature of the fiber alone, determining the principal directions of deformation for each mode is not feasible (refer to section 6.2).

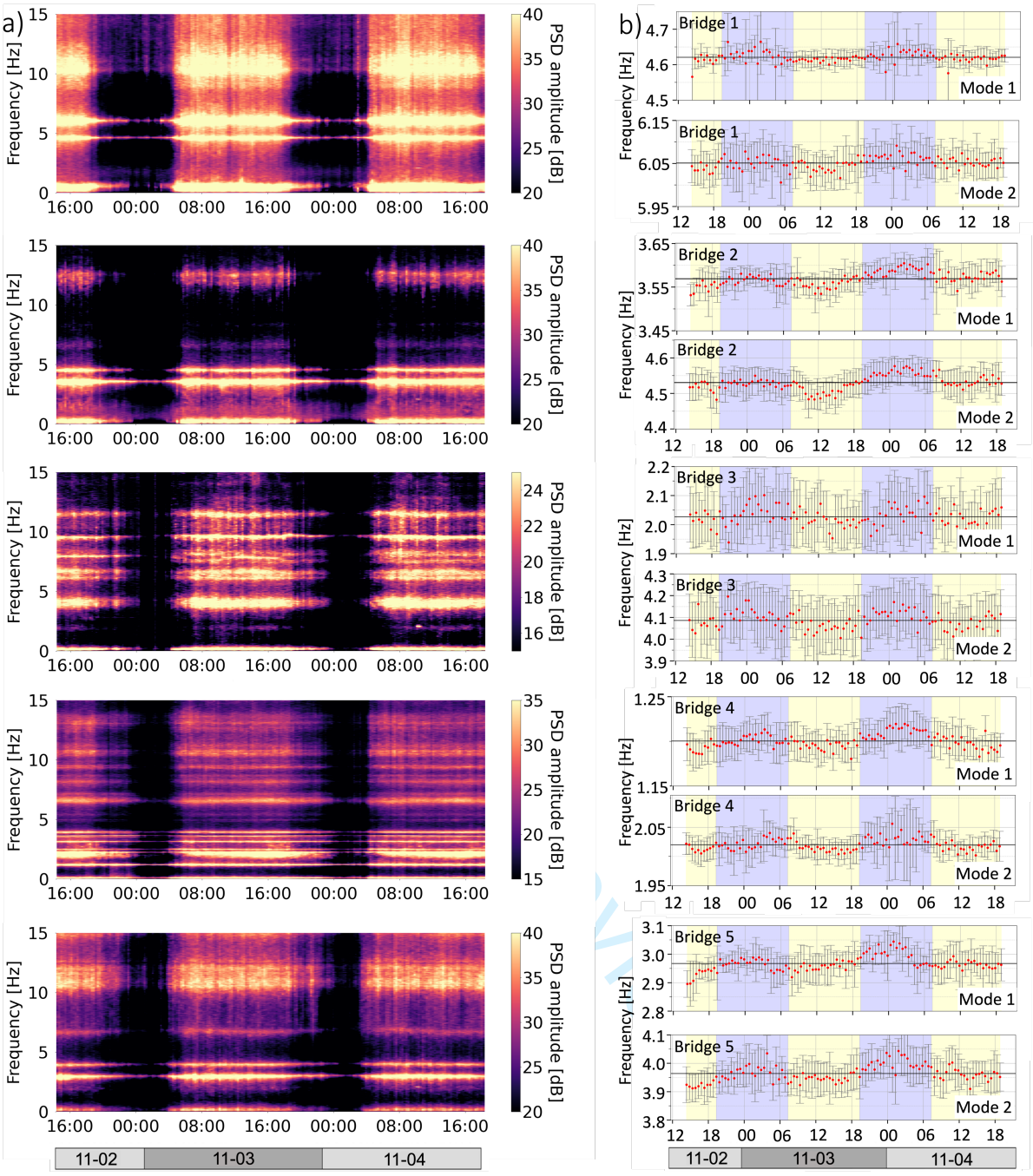

Figure 11: a) Spectrogram of each instrumented bridge. b) Frequency monitoring of the first two modes. Bridge 1: Paisy; Bridge 2: A6; Bridge 3: Saône; Bridge 4: Rhône; Bridge 5: Railway.

The Modal Assurance Criterion (MAC) index, reflecting the correlation between modal shapes for different modes, varies among bridges and reaches its minimum for the fundamental mode of bridge 2, with a low value of 0.787 (Figure 12b). Notably, across all bridges, the shape of the fundamental mode appears more susceptible to environmental variations compared to the

second mode (Figure 12b). For example, the shape of the second mode remains consistent for bridges 2 and 4 throughout the 53 hours of recording. In contrast, the shapes of the second mode for bridges 1 and 3 undergo some changes during the acquisition period. Additionally, it is observed that the shape of the fundamental mode for bridge 4 exhibits minimal variation over time, potentially attributed to its unique construction as the only steel bridge in the set.

Figures 11, 12, and Table 1 demonstrate that each bridge displays distinct dynamic behavior depending on factors such as its structure, materials, traffic conditions (higher ambient noise in the city center, hence more excited structures), and the environment (presence of rivers, highways, roads, railways), among others. This considerable variability underscores the importance of monitoring the dynamic behavior of each structure to ensure their safe operation by detecting or locating anomalies.

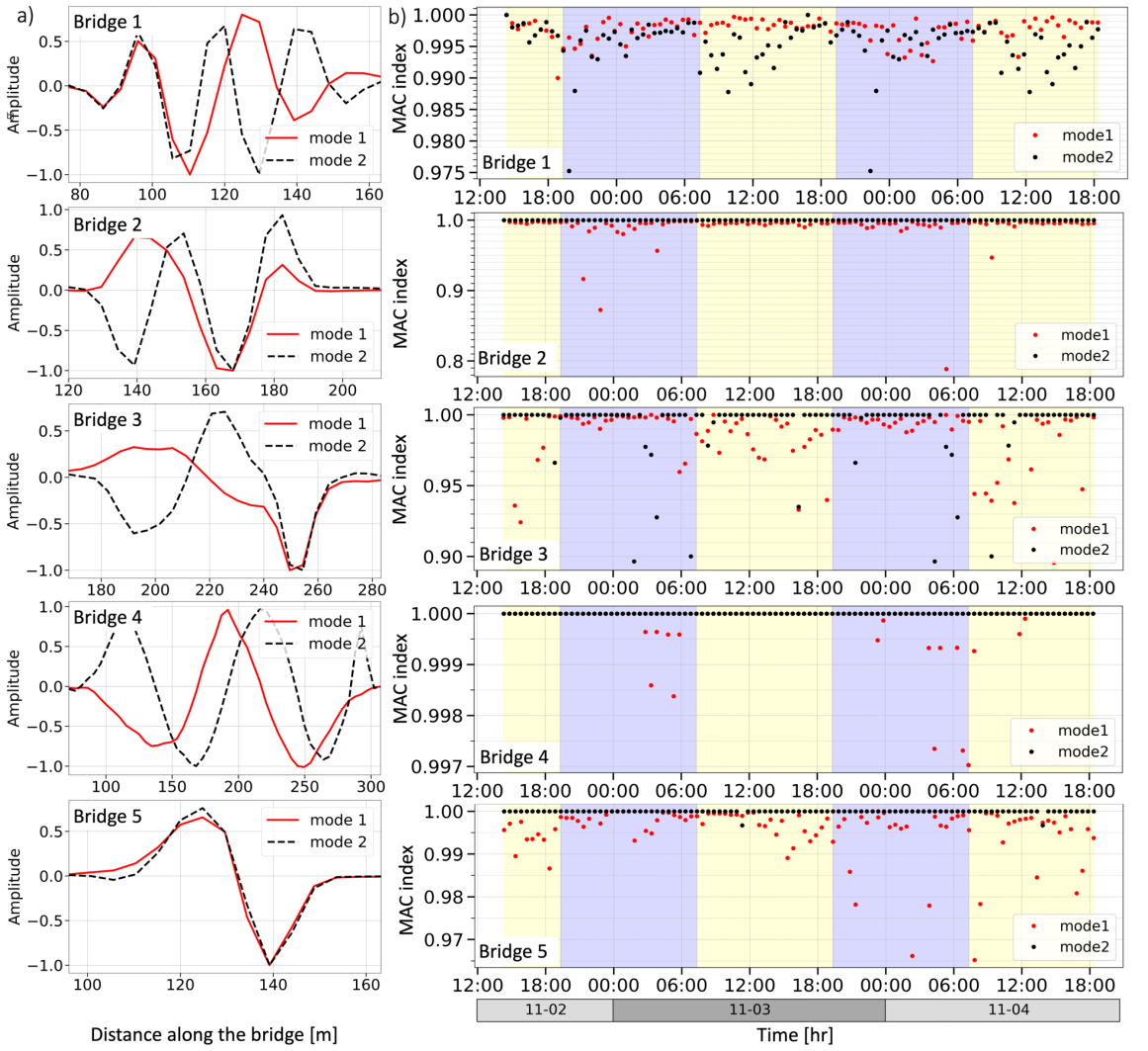

Figure 12: a) Modal shapes and b) MAC index of the first two modes reconstructed for each bridge. Bridge 1: Paisy; Bridge 2: A6; Bridge 3: Saône; Bridge 4: Rhône; Bridge 5: Railway.

6. Discussion

The telecom fiber enables the measurement of the dynamic response of bridges in the same way as synchronous acquisition from point velocimeters. Modal parameters obtained from the fiber and velocimeters are nearly identical (Table 1), and modal detection remains stable over time (Figure 8). However, the noise level in the fiber data is slightly higher. We constrain the signal to noise ratio (SNR) by measuring the ratio of the amplitude of the first resonance peak at 4.6Hz with respect to the base level. For bridge 1, this SNR from the fiber is approximately 85% of that of the velocimetric measurements. This observation testifies to the good sensitivity of the telecom fiber.

In contrast to frequency, the amplitude of the bridge modes undergoes fluctuations corresponding to the intensity of anthropogenic activities before stabilizing at night. Daily variations in vibration sources, predominantly traffic, lead to significant differences in amplitudes within a same bootstrap sample (containing 100 average PSDs), introducing substantial measurement uncertainties during the day (Figure 7 c, d). This observation underscores the impact of external factors on amplitude behavior and emphasizes the need for careful consideration of anthropogenic influences in dynamic response analysis.

6.1 Mode reconstruction

The vibratory identity cards (Figure 5) reveal that the fiber's response shares similarities but differs in details from any of the velocimetric component responses. This suggests that the fiber records a combination of the three directional components. Additionally, based on the telecom fiber data (Figure 8), we can concurrently reconstruct vertical and transverse vibration modes. In light of the "vibratory identity cards" and the mode shapes of Bridge 1, it appears that the telecom optical fiber is capable of measuring deformations in various directions, including those orthogonal to the fiber's axial direction or the longitudinal axis of the bridge. Considering our results (Figures 8, 10-12), we can reasonably assume that we are capturing all the elongations and compressions of the fiber resulting from the 3D deformations of the structure. Since vibration modes of a structure are physically independent of each other, we effectively distinguish them (Figure 12a) within a composite signal where all the information is amalgamated.

This conclusion appears at odd with the usual intuition of DAS vibrations being measured in the single fiber axial direction. For instance in classical optic fiber-based earthquake seismology, it is commonly admitted that little energy from a teleseismic P-wave is recorded

on the fiber because the P-wave incidence is small and the wave polarization is almost orthogonal to the fiber direction. So how do we explain the ability to reconstruct modes in any direction? In the case of a bridge which is embedded on both sides, the structure deforms and stretches dynamically, which results in a change through time of the elongation of the structure. If the fiber is coupled to the structure, the fiber itself stretches accompanying the motion of the structure following its different modes. The fiber elongation then introduces a change in the path length of the light emitted by the DAS interrogator, and consequently a phase shift. By measuring this phase shift, the DAS therefore makes it possible to reconstruct the deformation modes of the structure in all directions.

6.2 Limitations

From the fiber alone, which is uniaxial, deducing the principal directions of deformation for each mode is not feasible. The fiber records a combination of components, complicating the identification of deformation modes. Achieving such identification would require, for instance, the utilization of a three-component translational sensor to determine the principal mode directions.

In contrast to accelerometric networks, measurements on telecom fiber lack precise localization on structures. Despite not providing exact information on the dynamic data's location, recordings along the optical fiber enable the estimation of the same dynamic parameters as those obtained with accelerometers. Even without access to the precise location of the information, continuous monitoring of parameters over time remains feasible, proving crucial for damage detection (Gueguen and Tiganescu, 2018). This approach offers significant advantages, allowing for the simultaneous monitoring of dynamic parameters across various spatially distributed structures in a single acquisition. Moreover, it leverages existing infrastructure, eliminating the need for field deployment.

The analysis of Bridge 1's vibratory characteristics, shown in Figure 5, highlights how the structure's deck connects with the underlying soil through its piles and foundation system. These connection areas coincide with the deck's least deformed sections, aligning with the bridge's pier positions. However, when comparing fiber and velocimeter data directly, discrepancies arise in the number and location of low amplitude nodes. Several factors contribute to these differences. We are comparing deformation measurements over a 10-meter gauge length with specific point measurements, making their spatial resolutions inherently mismatched. Also, the asynchronous nature of velocimeter and fiber data, influenced by different excitation sources and recording positions, can alter the nodes' count and position,

causing disparities. Moreover, when interpolating velocimeter and fiber data with distinct spatial samplings, aliasing effects might occur, affecting node positions. Additionally, while assuming the fiber aligns perfectly with the bridge's axis, variations in the cable's orientation within the network sheath might cause deviations. However, these potential offsets don't impede the measurement of cable elongation and compression due to structural deformation in various spatial directions, illustrated in Figure 8.

6.3 Temperature effects

Rayleigh backscattering in optical fibers is primarily influenced by temperature-induced variations in fiber length due to thermal expansion. As temperature changes, the fiber either expands or compresses, leading to local density and refractive index fluctuations along the cable, contributing to Rayleigh backscattering. The impact of temperature on Rayleigh backscattering in optical fibers is typically more pronounced at lower frequencies (Kreger et al., 2009; Leggett et al., 2022). Given our operational frequencies (> 1Hz) and the limited thermal amplitude during the experiment (8°C), variations in fiber length due to temperature can be considered negligible.

The observed frequency fluctuations of 1.4% and 2.1% for the first two modes of bridge 1 (Figure 7a, b) are in reasonnable agreement with the influence of temperature changes recorded in Lyon in November 2021, ranging between 6°C and 14°C. This amplitude variation is consistent with other experiments demonstrating frequency changes of less than 5% for temperature fluctuations of approximately 15°C (Wahab and De Roeck, 1997; Peeters and De Roeck, 2001). The slight increase in eigenmode frequencies and the decrease in damping during the night (Figure 7a, b, e, f) may indicate an elevation in the Young's modulus of the concrete, leading to an overall stiffening of the structure under lower temperatures (Peeters and De Roeck, 2001). However, it is crucial to note that the frequency-temperature relationship isn't universally applicable, as shown by studies on the Alamosa Canyon bridge (USA) by Cornwell et al. (1999) and Sohn et al. (1999). The sensitivity of modal parameters to climatic variations is structure-specific, necessitating the consideration and prediction of these variations to detect potential structural damage (Peeters and De Roeck, 2001; Gueguen and Tiganescu, 2018). Figure 7e, f illustrates reduced energy dissipation during the night. However, the overall variations in frequency (Figure 7a, b) and damping (Figure 7e, f) during the night are associated with low amplitude measurements (Figure 7c, d). Consequently, the small variations observed in modal parameters might also result from nonlinear effects on the structure.

The observation of normal day/night variations emphasizes the system's ability to detect changes in the elastic parameters of materials (concrete, surface course) due to temperature. Environmental effects have intentionally not been corrected to observe temperature-induced fluctuations and quantify the normal variation range of modal parameters for each structure. Studies on environmental effects on modal parameters, such as those by Cornwell et al. (1999), Fu et al. (2001), Peeters et al. (2001), and Liu et al. (2007), have similarly concluded that modal shapes are less sensitive to temperature effects than frequencies. Correction of temperature effects primarily applies to frequency measurements and can be implemented in both fiber and velocimetric measurements using correction models (Rohrmann et al., 2000; Sohn et al., 1999; Peeters and De Roeck, 2001; Cury and Cremona, 2010). However, these models become unnecessary in decision-making for Structural Health Monitoring once temperature effects have been experimentally characterized (Gueguen and Tiganescu, 2018).

7. Conclusion

We demonstrate that a single telecom optical fiber, without prior deployment and in a single acquisition, can efficiently monitor multiple bridges spatially distributed along the cable. Consequently, the established telecom networks serve as an effective means to assess the modal parameters of several structures simultaneously, providing insights into the health of bridges without the need for deploying numerous synchronous stations. This use of existing infrastructure is particularly advantageous in hard-to-access locations, such as urban areas. Ultimately, this approach is in line with the vision of the smart city of tomorrow, utilizing information and communication technologies to enhance the operation of structures and ensure user safety.

8. Acknowledgments

This work is part of the DASARA project (Distributed Acoustic Sensing Auvergne Rhône-Alpes) and is supported by the Auvergne Rhône-Alpes Region. It involves several economic actors including FEBUS Optics, COVAGE and the Metropole de Lyon. We thank the Metropole de Lyon and the Rhône Department for providing the DTM and the data concerning the Paisy bridge (Bridge 1). We would also like to thank Fabien Dubuffet for his help on hardware and data management procedures. P.G. and O.C. thank LabEx OSUG@2020 (Investissements d'avenir-ANR10LABX56).

9. References

Ajo-Franklin, J. B., Dou, S., Lindsey, N. J., Monga, I., Tracy, C., Robertson, M., ... & Li, X. (2019). Distributed acoustic sensing using dark fiber for near-surface characterization and broadband seismic event detection. *Scientific reports*, *9*(1), 1328.

Allemang, R.J. & Brown, D.L. (1982). A correlation coefficient for modal vector analysis. Proceedings of the 1st International Modal Analysis Conference, Orlando, FL, USA.

Anastasopoulos, D., De Roeck, G., & Reynders, E. P. (2021). One-year operational modal analysis of a steel bridge from high-resolution macrostrain monitoring: Influence of temperature vs. retrofitting. *Mechanical Systems and Signal Processing*, *161*, 107951.

Brossault, M. A., Roux, P., & Guéguen, P. (2018). The fluctuation–dissipation theorem used as a proxy for damping variations in real engineering structures. *Engineering Structures*, *167*, 65-73.

Brownjohn, J. M. W., Magalhaes, F., Caetano, E., & Cunha, A. (2010). Ambient vibration re-testing and operational modal analysis of the Humber Bridge. *Engineering Structures*, *32*(8), 2003-2018.

Calvi, G. M., Moratti, M., O'Reilly, G. J., Scattarreggia, N., Monteiro, R., Malomo, D., ... & Pinho, R. (2019). Once upon a time in Italy: The tale of the Morandi Bridge. *Structural Engineering International*, *29*(2), 198-217.

Cao, R., El-Tawil, S., & Agrawal, A. K. (2020). Miami pedestrian bridge collapse: Computational forensic analysis. *Journal of Bridge Engineering*, *25*(1), 04019134.

Carini, M. R., & Rocha, M. M. (2022). CESSIPy: A Python open-source module for stochastic system identification in civil engineering. *SoftwareX*, *18*, 10109

Chatelain, J. L., Guillier, B., Gueguen, P., Fréchet, J., & Sarrault, J. (2012). Ambient vibration recording for single-station, array and building studies made simple: CityShark II. *International Journal of Geosciences*, *3*, 1168-1175.

Chen, W., Jin, M., Huang, J., Chen, Y., & Song, H. (2021). A method to distinguish harmonic frequencies and remove the harmonic effect in operational modal analysis of rotating structures. *Mechanical Systems and Signal Processing*, *161*, 107928.

Clough, R. W., and J. Penzien (1993). Dynamics of Structures, McGraw- Hill, New-York, 2nd edition, 768 pp., ISBN-10 0071132414,

Cole Jr, H. A. (1973). *On-line failure detection and damping measurement of aerospace structures by random decrement signatures* (No. NASA-CR-2205). NASA.

Cornwell, P., Farrar, C. R., Doebling, S. W., & Sohn, H. (1999). Environmental variability of modal properties. *Experimental techniques*, *23*(6), 45-48.

Cunha, Á., & Caetano, E. (2006). Experimental modal analysis of civil engineering structures.

Cunha, Á., Caetano, E., Magalhães, F., & Moutinho, C. (2018). Dynamic identification and continuous dynamic monitoring of bridges: different applications along bridges life cycle. *Structure and Infrastructure Engineering*, *14*(4), 445-467.

Cury, A., & Crémona, C. (2010). Long term dynamic monitoring of a PSC box girder bridge. In IABSE Symposium: Large Structures and Infrastructures for Environmentally Constrained and Urbanised Areas, Venice, Italy, 22-24 September 2010 (pp. 484-485).

Doebling, S. W., Farrar, C. R., Prime, M. B., & Shevitz, D. W. (1996). Damage identification and health monitoring of structural and mechanical systems from changes in their vibration characteristics: a literature review.

Dou, S., Lindsey, N., Wagner, A. M., Daley, T. M., Freifeld, B., Robertson, M., ... & Ajo-Franklin, J. B. (2017). Distributed acoustic sensing for seismic monitoring of the near surface: A traffic-noise interferometry case study. *Scientific reports*, *7*(1), 11620.

Efron, B., & Tibshirani, R. (1991). Statistical data analysis in the computer age. *Science*, *253*(5018), 390-395.

Ernst, R., Lauridsen, P., Klein, C., & Buffetti, B. (2022, May). The effect of damage position on Operational Modal Analysis of wind turbine blades for SHM. In *Journal of Physics: Conference Series* (Vol. 2265, No. 3, p. 032099). IOP Publishing.

Farrar, C. R., Doebling, S. W., & Nix, D. A. (2001). Vibration–based structural damage identification. *Philosophical Transactions of the Royal Society of London. Series A: Mathematical, Physical and Engineering Sciences*, *359*(1778), 131-149.

Farrar, C. R., & Worden, K. (2007). An introduction to structural health monitoring. *Philosophical Transactions of the Royal Society A: Mathematical, Physical and Engineering Sciences*, *365*(1851), 303-315.

Fichtner, A., Bogris, A., Nikas, T., Bowden, D., Lentas, K., Melis, N. S., ... & Smolinski, K. (2022). Theory of phase transmission fibre-optic deformation sensing. *Geophysical Journal International*, *231*(2), 1031-1039.

Figueiredo, E., & Brownjohn, J. (2022). Three decades of statistical pattern recognition paradigm for SHM of bridges . *Structural Health Monitoring*, *21*(6), 3018-3054.

Froggatt, M., Soller, B., Gifford, D., & Wolfe, M. (2004, February). Correlation and keying of Rayleigh scatter for loss and temperature sensing in parallel optical networks. In *Optical fiber communication conference* (p. PD17). Optica Publishing Group.

Fu, Y., & DeWolf, J. T. (2001). Monitoring and analysis of a bridge with partially restrained bearings. *Journal of Bridge Engineering*, *6*(1), 23-29.

Gara, F., Regni, M., Roia, D., Carbonari, S., & Dezi, F. (2019). Evidence of coupled soil-structure interaction and site response in continuous viaducts from ambient vibration tests. *Soil Dynamics and Earthquake Engineering*, *120*, 408-422.

García-Macías, E., & Ubertini, F. (2021). Structural assessment of bridges through ambient noise deconvolution interferometry: application to the lateral dynamic behaviour of a RC multi-span viaduct. *Archives of Civil and Mechanical Engineering*, *21*(3), 123.

Gifford, D. K., Kreger, S. T., Sang, A. K., Froggatt, M. E., Duncan, R. G., Wolfe, M. S., & Soller, B. J. (2007, October). Swept-wavelength interferometric interrogation of fiber Rayleigh scatter for distributed sensing applications. In *Fiber Optic Sensors and Applications V* (Vol. 6770, pp. 106-114). SPIE.

Glisic, B., & Inaudi, D. (2012). Development of method for in-service crack detection based on distributed fiber optic sensors. *Structural Health Monitoring*, *11*(2), 161-171.

Guéguen, P., Johnson, P., & Roux, P. (2016). Nonlinear dynamics induced in a structure by seismic and environmental loading. *The Journal of the Acoustical Society of America*, *140*(1), 582-590.

Guéguen, P., & Tiganescu, A. (2018). Consideration of the effects of air temperature on structural health monitoring through traffic light-based decision-making tools. *Shock and Vibration*, *2018*.

Hartog, A., Frignet, B., Mackie, D., & Clark, M. (2014). Vertical seismic optical profiling on wireline logging cable. *Geophysical Prospecting*, *62*(4-Vertical Seismic Profiling and Microseismicity Frontiers), 693-701.

Hartog, A. H., Belal, M., & Clare, M. A. (2018). Advances in distributed fiber-optic sensing for monitoring marine infrastructure, measuring the deep ocean, and quantifying the risks posed by seafloor hazards. *Marine Technology Society Journal*, *52*(5), 58-73.

Hearn, G., & Testa, R. B. (1991). Modal analysis for damage detection in structures. *Journal of structural engineering*, *117*(10), 3042-3063.

Jacobsen, N. J., Andersen, P., & Brincker, R. (2007). Eliminating the influence of harmonic components in operational modal analysis. In *Conference Proceedings: IMAC-XXIV: A Conference & Exposition on Structural Dynamics*. Society for Experimental Mechanics.

Jeary, A. P. (1997). Damping in structures. *Journal of wind engineering and industrial aerodynamics*, *72*, 345-355.

Johannessen, K., Drakeley, B., & Farhadiroushan, M. (2012, March). Distributed acoustic sensing-a new way of listening to your well/reservoir. In *SPE Intelligent Energy International Conference and Exhibition* (pp. SPE-149602). SPE.

Jousset, P., Reinsch, T., Ryberg, T., Blanck, H., Clarke, A., Aghayev, R., ... & Krawczyk, C. M. (2018). Dynamic strain determination using fibre-optic cables allows imaging of seismological and structural features. *Nature communications*, *9*(1), 2509.

Khoo, L. M., Mantena, P. R., & Jadhav, P. (2004). Structural damage assessment using vibration modal analysis. *Structural Health Monitoring*, *3*(2), 177-194.

Kreger, S. T., Sang, A. K., Gifford, D. K., & Froggatt, M. E. (2009, April). Distributed strain and temperature sensing in plastic optical fiber using Rayleigh scatter. In *Fiber Optic Sensors and Applications VI* (Vol. 7316, pp. 85-92). SPIE.

Leggett, S. E., Zhu, D., & Hill, A. D. (2022). Thermal effects on far-field distributed acoustic strain-rate sensors. *SPE Journal*, *27*(02), 1036-1048.

Lindsey, N. J., Dawe, T. C., & Ajo-Franklin, J. B. (2019). Illuminating seafloor faults and ocean dynamics with dark fiber distributed acoustic sensing. *Science*, *366*(6469), 1103-1107.

Liu, C., & DeWolf, J. T. (2007). Effect of temperature on modal variability of a curved concrete bridge under ambient loads. *Journal of structural engineering*, *133*(12), 1742-1751.

Magalhães, F., Cunha, Á., & Caetano, E. (2008). Dynamic monitoring of a long span arch bridge. *Engineering Structures*, *30*(11), 3034-3044.

Magalhães, F., & Cunha, Á. (2011). Explaining operational modal analysis with data from an arch bridge. *Mechanical systems and signal processing*, *25*(5), 1431-1450.

Magalhães, F., Cunha, Á., & Caetano, E. (2012). Vibration based structural health monitoring of an arch bridge: From automated OMA to damage detection. *Mechanical Systems and signal processing*, *28*, 212-228.

Mateeva, A., Lopez, J., Potters, H., Mestayer, J., Cox, B., Kiyashchenko, D., ... & Detomo, R. (2014). Distributed acoustic sensing for reservoir monitoring with vertical seismic profiling. *Geophysical Prospecting*, *62*(4-Vertical Seismic Profiling and Microseismicity Frontiers), 679-692.

Maurey, H., Chaize, P., & Dagbert, M. (2019). Sécurité des ponts : Éviter un drame.

Mestayer, J., Cox, B., Wills, P., Kiyashchenko, D., Lopez, J., Costello, M., ... & Lewis, A. (2011). Field trials of distributed acoustic sensing for geophysical monitoring. In *Seg technical program expanded abstracts 2011* (pp. 4253-4257). Society of Exploration Geophysicists.

Michel, C., Guéguen, P., El Arem, S., Mazars, J., & Kotronis, P. (2010). Full-scale dynamic response of an RC building under weak seismic motions using earthquake recordings, ambient vibrations and modelling. *Earthquake Engineering & Structural Dynamics*, *39*(4), 419-441.

Mikael, A., Gueguen, P., Bard, P. Y., Roux, P., & Langlais, M. (2013). The analysis of long-term frequency and damping wandering in buildings using the random decrement technique. *Bulletin of the Seismological Society of America*, *103*(1), 236-246.

Peeters, B., & De Roeck, G. (2001). One-year monitoring of the Z24-Bridge: environmental effects versus damage events. *Earthquake engineering & structural dynamics*, *30*(2), 149-171.

Peeters, B., Maeck, J., & De Roeck, G. (2001). Vibration-based damage detection in civil engineering: excitation sources and temperature effects. *Smart materials and Structures*, *10*(3), 518.

Rao, C. R., Rao, C. R., Statistiker, M., Rao, C. R., & Rao, C. R. (1973). *Linear statistical inference and its applications* (Vol. 2, pp. 263-270). New York: Wiley.

Rizzo, P., & Milazzo, A. (Eds.). (2021). *European Workshop on Structural Health Monitoring: Special Collection of 2020 Papers-Volume 1* (Vol. 127). Springer Nature.

Rodrigues, J., & Brincker, R. (2005). Application of the random decrement technique in operational modal analysis. In *Proceedings of the 1st International Operational Modal Analysis Conference, April 26-27, 2005, Copenhagen, Denmark* (pp. 191-200). Aalborg Universitet.

Roeck, G. D. (2003). The state-of-the-art of damage detection by vibration monitoring: the SIMCES experience. *Journal of Structural Control*, *10*(2), 127-134.

Rohrmann, R. (2000). Structural causes of temperature affected modal data of civil structures obtained by long time monitoring.

Sladen, A., Rivet, D., Ampuero, J. P., De Barros, L., Hello, Y., Calbris, G., & Lamare, P. (2019). Distributed sensing of earthquakes and ocean-solid Earth interactions on seafloor telecom cables. *Nature communications*, *10*(1), 5777.

Snover, D., Johnson, C. W., Bianco, M. J., & Gerstoft, P. (2021). Deep clustering to identify sources of urban seismic noise in Long Beach, California. *Seismological Society of America*, *92*(2A), 1011-1022.

Sohn, H., Dzwonczyk, M., Straser, E. G., Kiremidjian, A. S., Law, K. H., & Meng, T. (1999). An experimental study of temperature effect on modal parameters of the Alamosa Canyon Bridge. *Earthquake engineering & structural dynamics*, *28*(8), 879-897.

Song, Z., Zeng, X., Xie, J., Bao, F., & Zhang, G. (2021). Sensing shallow structure and traffic noise with fiber-optic internet cables in an urban area. *Surveys in Geophysics*, *42*, 1401-1423.

Tanimola, F., & Hill, D. (2009). Distributed fibre optic sensors for pipeline protection. *Journal of Natural Gas Science and Engineering*, *1*(4-5), 134-143.

Van den Ende, M., Ferrari, A., Sladen, A., & Richard, C. (2022). Deep Deconvolution for Traffic Analysis with Distributed Acoustic Sensing Data. *IEEE Transactions on Intelligent Transportation Systems*.

Van Overschee, P., & De Moor, B. (1996). Continuous-time frequency domain subspace system identification. *Signal Processing*, *52*(2), 179-194.

Wahab, M. A., & De Roeck, G. (1997). Effect of temperature on dynamic system parameters of a highway bridge. *Structural Engineering International*, *7*(4), 266-270.

Wang, H. F., Zeng, X., Miller, D. E., Fratta, D., Feigl, K. L., Thurber, C. H., & Mellors, R. J. (2018). Ground motion response to an ML 4.3 earthquake using co-located distributed acoustic sensing and seismometer arrays. *Geophysical Journal International*, *213*(3), 2020-2036.

Welch, P. (1967). The use of fast Fourier transform for the estimation of power spectra: a method based on time averaging over short, modified periodograms. *IEEE Transactions on audio and electroacoustics*, *15*(2), 70-73.

Xia, Y., & Hao, H. (2003). Statistical damage identification of structures with frequency changes. *Journal of Sound and Vibration*, *263*(4), 853-870.

Zeng, X., Lancelle, C., Thurber, C., Fratta, D., Wang, H., Lord, N., ... & Clarke, A. (2017). Properties of noise cross-correlation functions obtained from a distributed acoustic sensing array at Garner Valley, California. *Bulletin of the Seismological Society of America*, *107*(2), 603-610.